

다이아몬드막의 광전도성에 관한 수소 플라즈마 표면 처리의 효과

김성훈
신라대학교 신소재 화학전공, 부산, 617-736

Effect of Hydrogen Plasma Treatment on the Photoconductivity of Free-standing Diamond Film

Sung-Hoon, Kim

Chemistry of New Materials, Silla University, Sasang-gu, Pusan 617-736, Korea

요 약 몰리브데늄 기판과 4 kW의 고출력 마이크로웨이브 플라즈마 증착 장치를 이용하여 약 700 μm 의 두께를 갖는 다이아몬드 막을 증착 하였다. 증착된 다이아몬드 막과 몰리브데늄 기판을 진공상태에서 빠르게 냉각시킴으로 잘 분리된 다이아몬드 자체 막을 쉽게 얻을수 있었다. 산소 또는 수소의 플라즈마로 다이아몬드 막의 표면을 처리한후, 다이아몬드 막의 광전도 현상을 측정하였다. 표면 처리하기 전의 다이아몬드막 성장 표면은 광전도 현상을 나타내었으나 막 표면에 산소 플라즈마 처리를 실시한 결과 다이아몬드 막은 절연체로 변하였다. 반면, 수소 플라즈마로 다시 처리한 결과 다이아몬드 막은 광전도성을 잘 나타내었다. 이러한 결과들로부터 다이아몬드 막의 광전도성은 수소 플라즈마를 처리함으로 잘 생성 됨을 알 수 있었다.

Abstract Thick diamond film having $\sim 700 \mu\text{m}$ thickness was deposited on polycrystalline molybdenum (Mo) substrate using high power (4 kW) microwave plasma-enhanced chemical vapor deposition (MPECVD) system. We could achieve free-standing diamond film via detaching as-deposited diamond film from the substrate by rapid cooling them under vacuum. We investigated the variation of photoconductivity after exposing the film surface to either oxygen or hydrogen plasma. At as-grown state, the growth side (the as-grown surface of the film) showed noticeable photoconductivity. The oxygen plasma treatment of this side led to the insulator. After exposing the film surface to hydrogen plasma, on the other hand, we could observe the reappearing of photoconductivity at the growth side. Based on these results, we suggest that the hydrogen plasma treatment may enhance the photoconductivity of free-standing diamond film

Introduction

Below picosecond transient photoconductive phenomenon using high-resistive semiconductor materials provides a unique method for fabricating an ultra-fast and high-voltage optoelectronic switches. Among the high-resistive semiconductor materials, the diamond has been noticed as a promising material because of its superior characteristics, such as highest breakdown voltage (10^7 V/cm), high resistance (10^{16} Ω cm), and small dielectric constant (5.5) [1-3]. Switching time of optoelectronic switches was composed of the signal rising and falling time. In the case of diamond single crystal, the falling time was known to be much longer (> 3 times) than that of the rising time [4, 5]. It means that the bottleneck for ultra-fast switching time may be the falling time. The falling time would be affected by the carrier lifetime. Therefore, we can decrease the falling time by using a polycrystalline diamond film, instead of a diamond single crystal, because the carrier lifetime can be reduced via controlling grain boundary and impurity concentration. Consequently, the ultra-fast and high-voltage optoelectronic switches can be fabricated merely by using polycrystalline diamond film.

In this work, we fabricated parallel-type Ohmic-contacted diamond photoconductors using free-standing polycrystalline diamond films. Prior to fabricating the photoconductors, we treated the growth side using oxygen and/or hydrogen plasma. The variation of the morphologies and the diamond qualities were investigated as a function of surface treatments. Finally, we can confirm the occurrence of photoconductivity for free-standing diamond films, merely treated by hydrogen plasma, which will be applicable to ultra-fast optoelectronic switches.

Experimental

For obtaining thick free-standing diamond films, first of all, we deposited diamond films with a thickness of about 700 μm on 2" polycrystalline Mo (99.9 %) discs in a MPECVD (5kW) system. In this case, we used mixtures of 5% methane, 0.4% oxygen in hydrogen as a total gas flow rate at 500 sccm. Total pressure was 100 Torr. Microwave power and growth time was 4 kW and 100 h, respectively. The substrate, placed on the Mo substrate holder, was merely heated by the plasma. After depositing the film, we separate the film from substrate. Detailed process will be presented and discussed in Results & discussion.

The conditions for the surface plasma treatments of free-standing diamond films are as follows: total gas flow rate = 200 sccm, total pressure = 40 Torr, microwave power = 1,000 watt, and reaction time = 3 min, respectively. Characteristics were investigated using scanning electron microscopy (SEM) and micro-Raman spectroscopy.

For fabricating diamond photoconductors, we deposited circular-type Au/Ti electrodes (4 mm spacing, $0.2 \times 0.2 \text{ mm}^2$ area) onto the free-standing diamond films using direct current (DC) sputtering system. The thickness of Au and Ti were 1,400 and 1,000 \AA , respectively. For making Ohmic-contacts between the electrodes and the films, we annealed (at 750 $^{\circ}\text{C}$) the electrode-deposited films in hydrogen gas for 30 minutes. Ohmic-contacts were confirmed via current to voltage (I-V) measurements in the bias voltage range of -10 V to + 10 V. White light of tungsten lamp without monochromator was used as a light source to observe the photoconductivity as a function of the light on/off. The lamp power was calibrated using optical power meter (Newport 840) in the range of 400 ~ 1,100 nm wavelength. Tungsten lamp had a strong optical power around 400 nm (Blue region) and 1,100 nm (near IR). Static photoconductive spectra were also obtained using 1,000 watt Xe lamp, 1/4" monochromator and source-measuring unit (Keithley 236).

Results and Discussion

Prior to making diamond photoconductors, we fabricated free-standing diamond films as follows. For readily obtaining free-standing diamond films from the Mo substrate, we engraved micro-grooved lines (width = ~ 0.3 mm, depth = ~ 1.0 mm) on the 3 mm thick Mo substrate using precision drill. After growing a diamond film on the engraved Mo substrate, the substrate was rapidly cooled down (~ 50 °C/min) under vacuum. Then, we softly beat the edges of the micro-grooves with a small hammer. In this way, we could easily detach diamond films from the Mo substrate [6]. We believe that the cause for this was mainly due to the large difference of thermal expansion coefficient between them [7].

Then, we investigated the effect of surface treatments on the surface morphologies and the diamond qualities of the free-standing diamond films. The morphology transitions of the growth side (Fig. 1) accompanied with surface treatments were examined using SEM. After hydrogen plasma treatment, we can not distinctly observe the morphology changes from the as-grown states (compare Figs. 1a with b). After oxygen plasma treatment, however, we can clearly observe the abrupt changes of surface morphologies (see Fig. 1c). In addition, the changed morphologies show the deterioration of surface morphologies, namely, a great deal of grains, void formations, coarse surface states, and so forth. Consequently, we conjecture the decrease of the photoconductivity for the film treated by oxygen plasma, due to the deterioration of the surface morphologies. The films, already treated with oxygen plasma, were also carried out the hydrogen plasma treatment (see Fig. 1d). In this case, we can observe the macroscopic restoration of the morphologies. In addition, we imagine a little microscopic smoothing effect for the surface morphologies by hydrogen plasma treatment (closely compare Figs. 1c and d). Obviously, these results reveal that the hydrogen plasma treatment does not give a critical detrimental effect for the surface morphology.

The variation of diamond qualities for the free-standing diamond films after surface treatments were examined using Raman spectroscopy as shown in Fig. 2. We first examine the diamond qualities at as-grown state. As shown in Fig. 2, the growth side and the substrate side (surface of the film detached from Mo substrate) give the sharp diamond intrinsic peak ($\sim 1332 \text{ cm}^{-1}$) with little nondiamond characteristic peaks (around $\sim 1500 \text{ cm}^{-1}$), respectively. These results reveal the existence of good diamond quality at each side. In addition, we can not observe any obvious variation in the Raman spectra as functions of surface treatments (see Fig. 3). Not only the value ($\sim 6.3 \text{ cm}^{-1}$) of full width at half maximum (FWHM) but also the position ($\sim 1332 \text{ cm}^{-1}$) of diamond intrinsic peak did not changed. These results reveal that the surface treatments using hydrogen or oxygen plasma give little effect for the diamond quality. From the combined results of Figs. 1 ~ 3, we may conclude that merely the oxygen plasma treatment can invoke the deterioration of the surface morphology with little effect on the diamond quality.

For the diamond photoconductors, Au/Ti electrodes were Ohmic-contacted onto the each side as a parallel-type. We measured the current variation between the electrodes during short time exposing the films to tungsten (W) light. At as-grown state, the growth side showed the photoconductivity with $\sim 0.6 \%$ photo/dark-current ratio (the measured current ratio of light on to light off) (see Fig. 4). After hydrogen plasma treatment, we could observe the similar photoconductive behavior with that of as-grown state. After oxygen plasma treatment, however, we could not observe the photoconductivity (see Fig. 5). It means the extinction of photoconductivity when exposing these films to oxygen plasma. Noticeably, the dark current level was lowered as $\sim 10^3$ times (from μA to pA), compared with that of as-grown state. In the case of oxygen plasma treatment, we might consider that the surface dangling bonds, hydrogen might be dangled at as-grown state, could be replaced by oxygen. Therefore we suggest that the surface morphology deterioration and/or surface dangling

bonds replacement as oxygen may be the main causes for the photoconductive extinction and the dark current level decrease. After oxygen plasma treatment, we treated again the same film using the hydrogen plasma. In this case we can clearly observe the reappearing of photoconductive (see Fig. 6) behavior. We might consider that the surface dangling bonds could be replaced again by hydrogen. Therefore we suggest that surface dangling bond characteristics may be a primary factor for the photoconductivity. Noticeably, we can observe the enhancement of the photo/dark-current ratio ($\sim 9.0\%$) about 15 times, compared with that ($\sim 0.6\%$) of the as-grown state of the film. This result strongly reveals that the oxygen \rightarrow hydrogen plasma treatments can enhance the photo/dark-current ratio in the photoconductivity. As shown in Fig 6, the dark current level was measured as around $\sim 4.0\ \mu\text{A}$. This value is ~ 20 times higher than that of the oxygen plasma treatment (compare Figs 5 with 6). However, this value is still ~ 60 times lower than that of as-grown state (compare Figs. 4 with 6). From these results, we can strongly confirm the occurrence of photoconductivity of the films related to the hydrogen plasma treatment.

Conclusions

The oxygen plasma treatment for the growth side of the film led to the insulators. However, the hydrogen plasma treatment for this side could give the photoconductive behavior. We suggest that the hydrogen-dangling bonds on the film surface may play an important role to create the photoconductivity. In addition, the oxygen \rightarrow hydrogen plasma treatments for each side can enhance the photo/dark current ratio

Acknowledgement

The author wish to acknowledge the financial support of the Korea Research Foundation made in the program year of (1998).

References

1. V. K. Bazhenov, I. V. Vikuolin and A. G. Gontar, *Sov. Phys. Semicond.*, 19 (1985) 829.
2. K. Shenai, R. S. Scott and B. J. Baliga, *IEEE Trans. Electron. Devices*, 36 (1989) 1811.
3. D.Kania, O. L. Landen, L. Pan, P. Pianetta and K. V. Ravi, *OSA Proc. on picosec. electron. and optoelectron.* 4 (1989) 170.
4. H. Yoneda and K. -i. Ueda, *Appl. Phys. Lett.*, 66(4) (1995) 460.
5. K. Baba, Y. Aikawa, N. Shohara, H. Yoneda, and K. -i. Ueda, *NEC Res. & Develop.*, 36(3) (1995) 369.
6. N. Francois, S. H. Kim, Y. S. Park, J.-W. Lee, I. T. Hahn, W. S. Yun, *Diamond Relat. Mater.*, 6 (1996) 959.
7. G. A. Slack and S. F. Bartram, *J. Appl. Phys.*, 46 (1975) 89.

Figure captions

Fig. 1 SEM images of the film surface for the growth side (a) at as-grown state, (b) after hydrogen plasma treatment, (c) after oxygen plasma treatment, and (d) after oxygen → hydrogen plasma treatment.

Fig. 2 Raman spectra of the film (a) for the substrate side and (b) for the growth side.

Fig. 3 Raman spectra of the film for the growth side (a) at as-grown state, (b) after oxygen plasma treatment, and (c) after hydrogen plasma treatment.

Fig. 4 Current variation between the electrodes, during short time exposing to tungsten light, on the growth side at as-grown state.

Inset shows the Ohmic contact behavior between the electrode and the film.

Fig. 5 Current variation between the electrodes, during short time exposing to tungsten light, on the growth side after oxygen plasma treatment.

Inset shows the Ohmic contact behavior between the electrode and the film.

Fig. 6 Current variation between the electrodes, during short time exposing to tungsten light, on the growth side after oxygen → hydrogen plasma treatment.

Inset shows the Ohmic contact behavior between the electrode and the film.

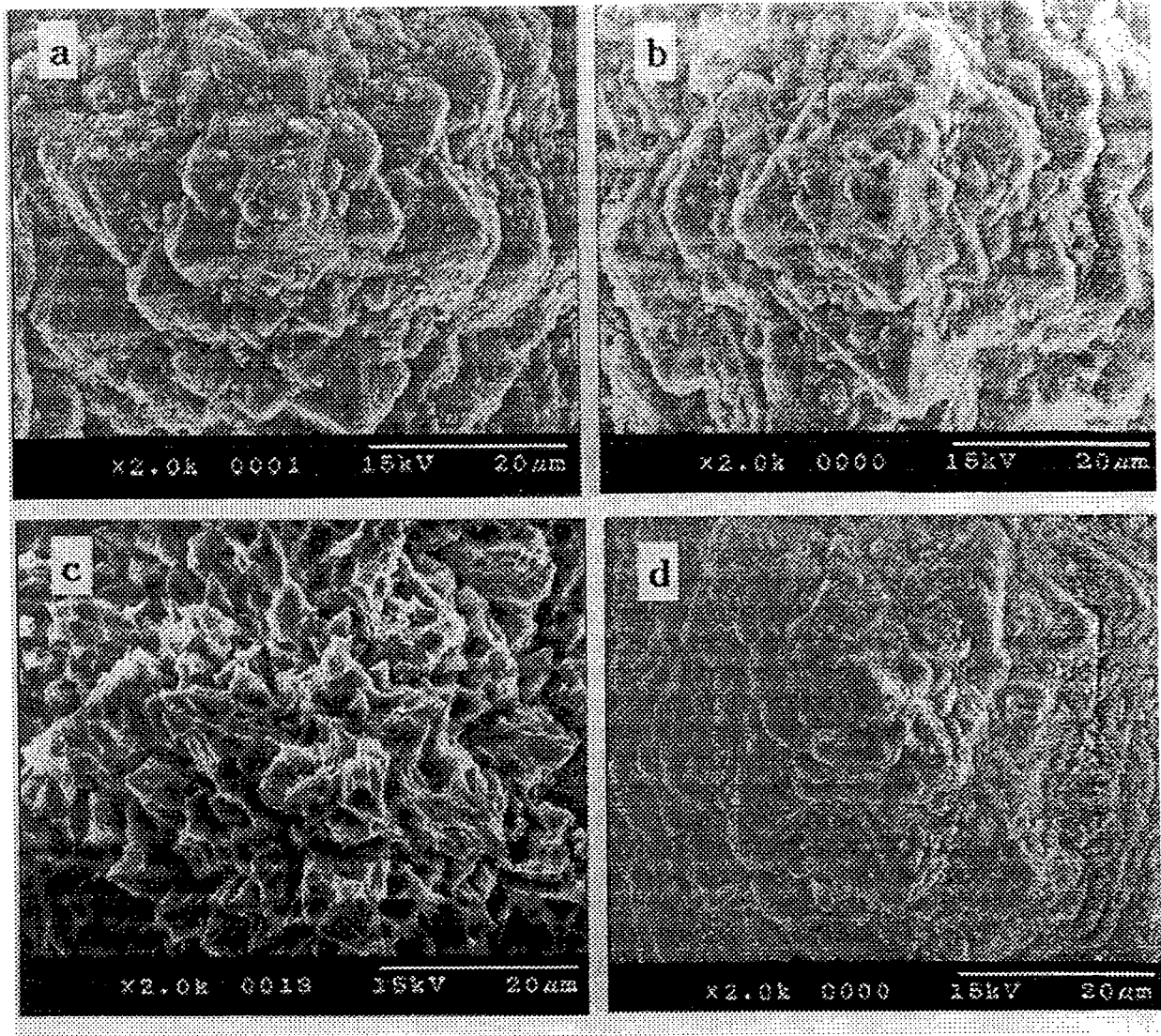
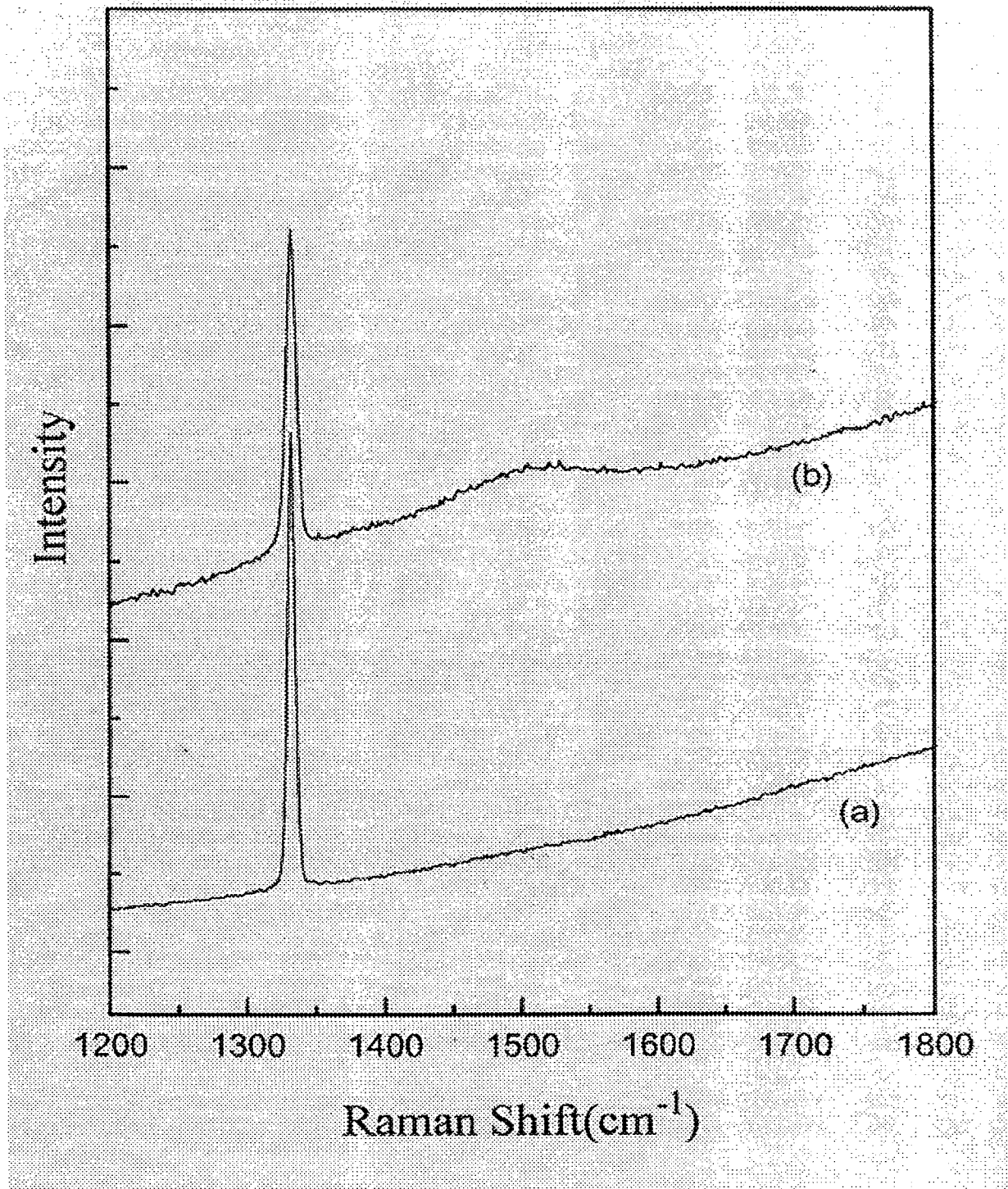


Fig. 1

*Fig. 2*

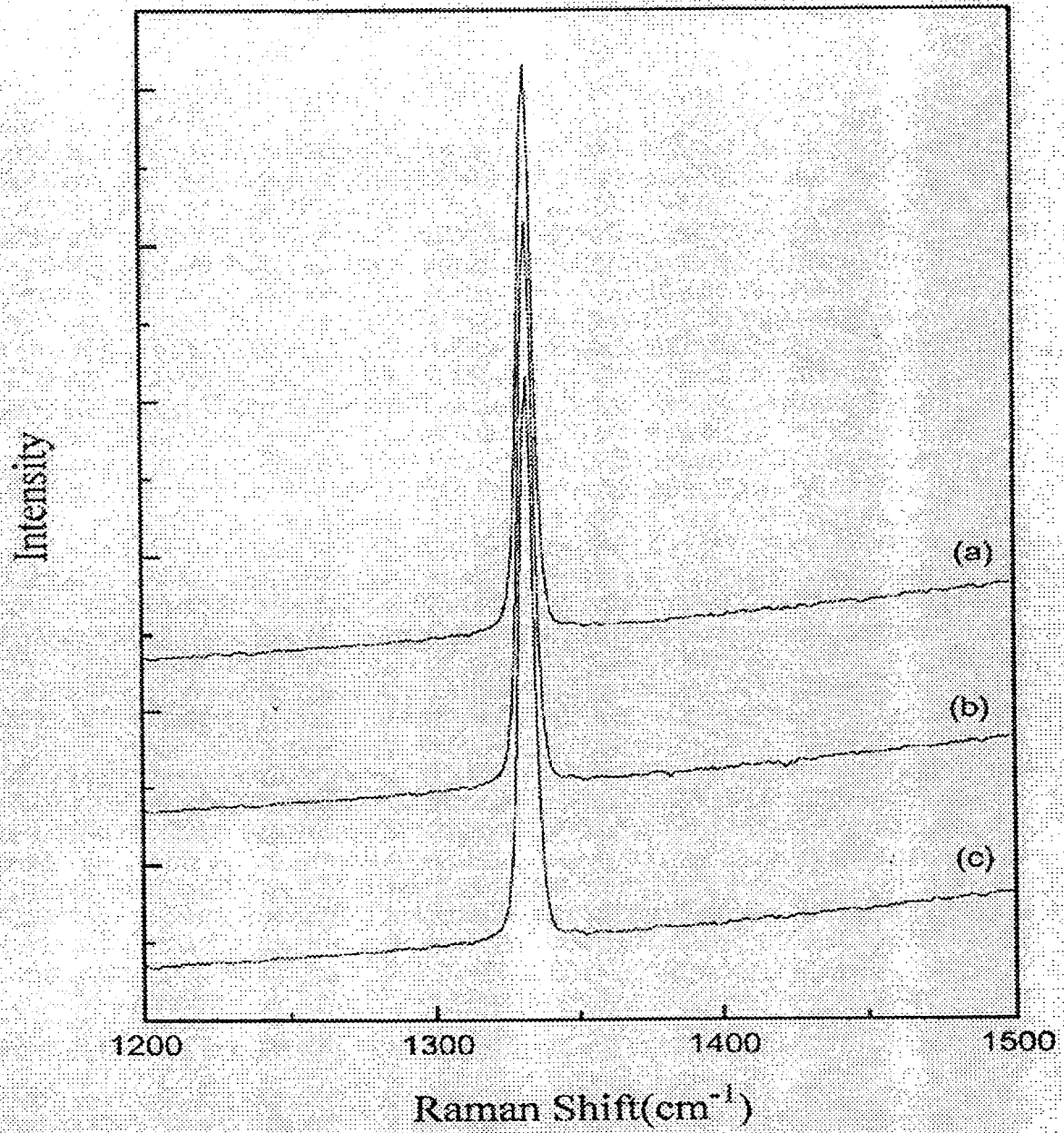
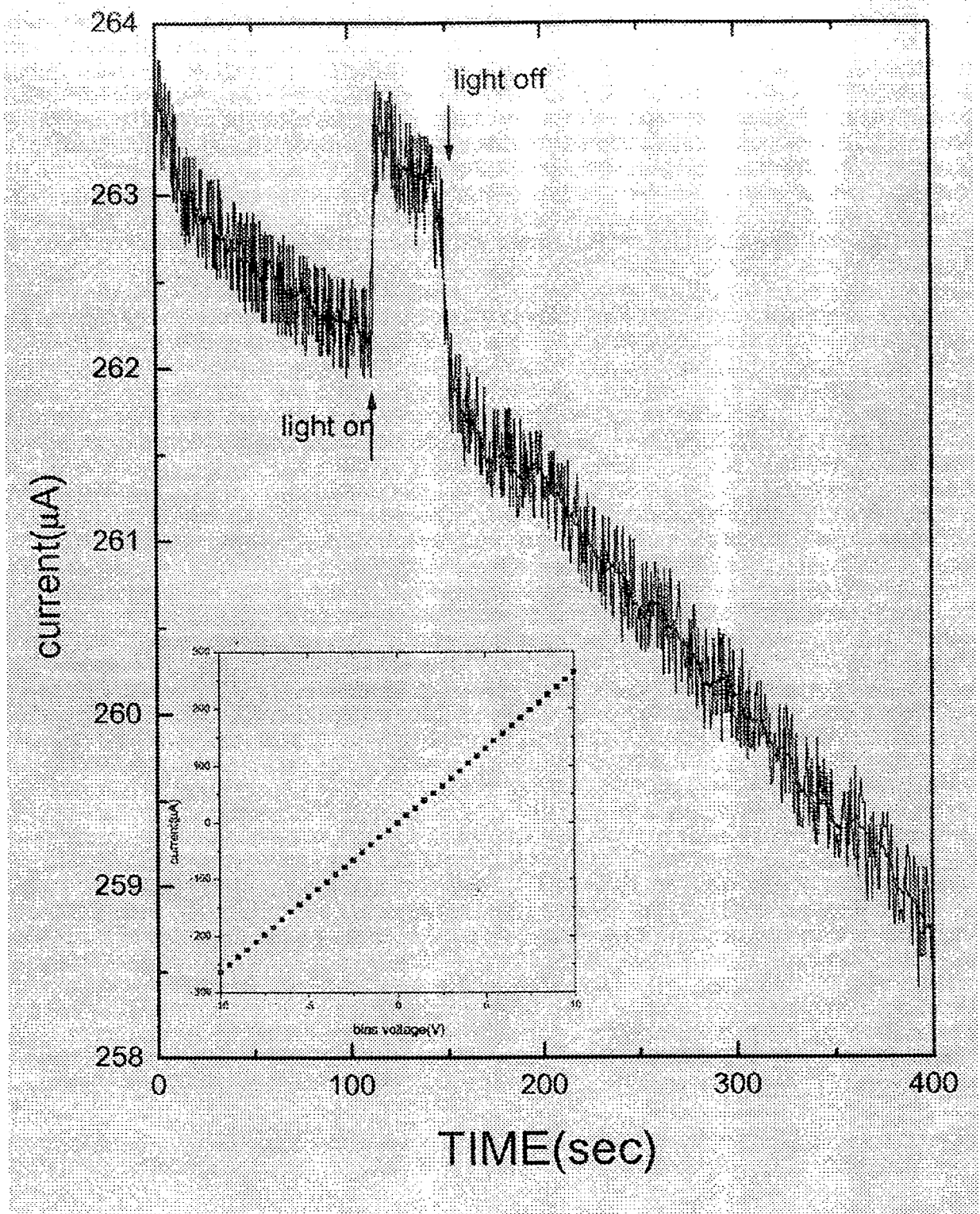


Fig. 3

*Fig. 4*

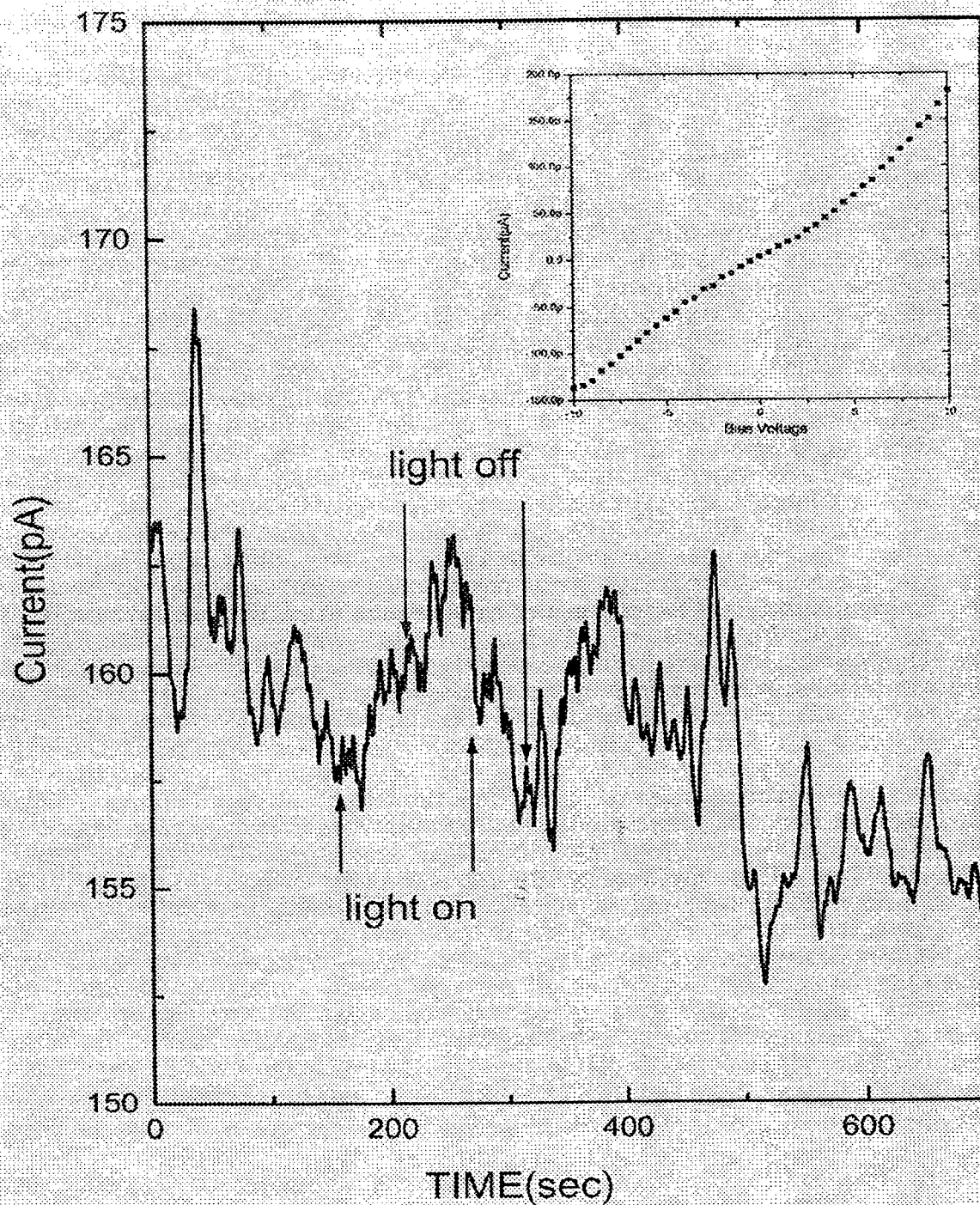
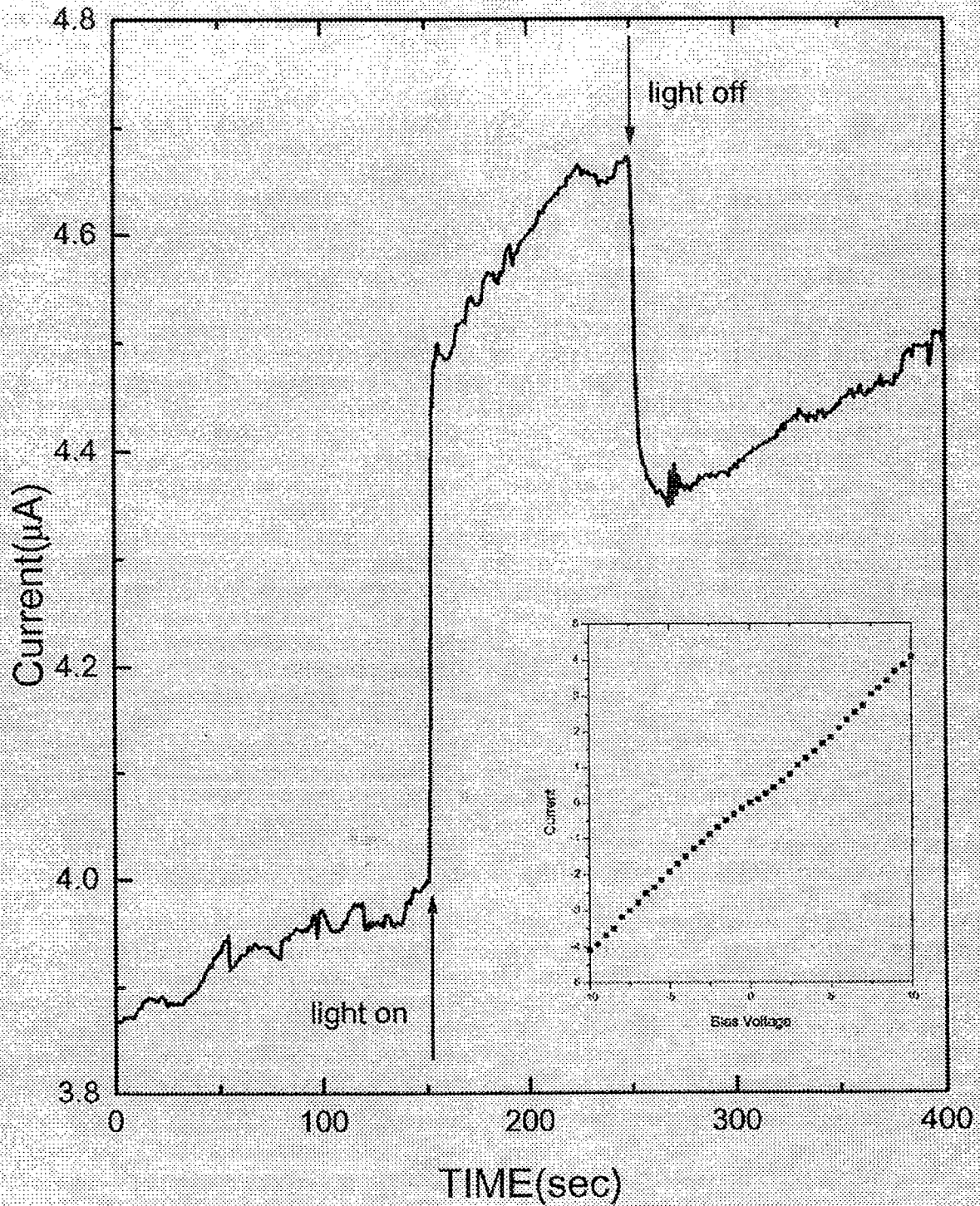


Fig. 5

**Fig. 6**